

Phylogeography, character evolution and taxonomy of Scurrulinae (Loranthaceae): New insights into the circumscription of the genus *Taxillus*

Chi Toan Le

Hanoi Pedagogical University 2

Limin Lu

Institute of Botany, Chinese Academy of Sciences

Van Du Nguyen

Institute of Ecology and Biological Resources (IEBR), Vietnam Academy of Science and Technology

Zhiduan Chen

Institute of Botany, Chinese Academy of Sciences

Wyckliffe Omondi Omollo

Institute of Botany, Chinese Academy of Sciences

Bing Liu (✉ liubing@ibcas.ac.cn)

Institute of Botany, Chinese Academy of Sciences

Research Article

Keywords: phylogeny, historical biogeography, Scurrulinae, Phyllodesmis, Africa, taxonomy, Asia

Posted Date: July 7th, 2023

DOI: <https://doi.org/10.21203/rs.3.rs-3111132/v1>

License: © ⓘ This work is licensed under a Creative Commons Attribution 4.0 International License.

[Read Full License](#)

Abstract

Background

Exploring the relationship between parasitic plants and answering taxonomic questions are still challenging. The subtribe Scurrulinae (Loranthaceae), which has a wide distribution in Asia and Africa, provides an excellent example to illuminate this scenario. Using a comprehensive taxon sampling of the subtribe, this study focuses to infer the phylogenetic relationships within Scurrulinae, investigate the phylogeography of the subtribe, and establish a phylogenetically-based classification incorporating both molecular and morphological evidence. We conducted phylogenetic, historical biogeography, and ancestral character state reconstruction analyses of Scurrulinae based on the sequences of 6 DNA regions from 89 individuals to represent all 5 tribes of the Loranthaceae and the dataset from eleven morphological characters.

Results

The results strongly support the non-monophyletic of Scurrulinae, with *Phyllodesmis* recognized as a separate genus from its allies *Taxillus* and *Scurrula*. "*Afrotaxillus*" is well supported as a new genus from Africa. The mistletoe Scurrulinae originated in Asia during the Oligocene. Scurrulinae was inferred to have been widespread in Asia but did not disperse to other areas. "*Afrotaxillus*" was confirmed to have originated in Africa from African Loranthaceae ca. 17 Ma, and likely the genus independently evolved from *Taxillus* in Asia.

Conclusions

This study based on comprehensive taxon sampling of the subtribe Scurrulinae, strongly supports the relationship between genera. The taxonomic treatment for *Phyllodesmis*, *Afrotaxillus* were provided. The historical biogeography of mistletoe Scurrulinae was determined with origin in Asia during the Oligocene. *Taxillus* and *Scurrula* diverged during the climatic optimum in the middle Miocene. *Afrotaxillus* originated in Africa from African Loranthaceae. Diversification of Scurrulinae and the development of endemic species in Asia may have been supported by the fast-changing climate, including cooling, drying, and the progressive uplift of the high mountains in central Asia, especially during the late Pliocene and Pleistocene.

Background

Loranthaceae is the largest mistletoe family within the order Santalales, comprising approximately 76 genera and over 1000 species. Species of the family are mainly distributed in tropical and subtropical regions of America, Africa, Asia, and Australia, with a few extending to the temperate zones in Europe and

East Asia [1–5]. The aerial parasitic species of Loranthaceae exhibit unique morphology with a haustorium connection structure that adds to the family's diversity worldwide.

The subtribe Scurrulinae, comprising *Scurrula* (ca. 50 spp.) and *Taxillus* (ca. 35 spp.), was established by Nickrent et al. [2] and recognized by Kuijt [4], Liu et al. [5] and Su et al. [6]. Most members of Scurrulinae are distributed in Asia, except for *Taxillus wiensii* Polhill, the sole species in Africa [7]. Several species of the two genera, such as *Taxillus delavayi* (Tieghem) Danser, *T. gracilifolius* (Schult.) T.B. Nguyen, *T. caloreas* (Diels) Danser, *T. renii* H.S. Kiu, *T. chinensis* (Candolle) Danser, and *Scurrula parasitica* L., are used as local medicines [4, 8].

The subfamily Scurrulinae has received limited taxonomic attention. Flora Reipublicae Popularis Sinicae identified 26 species of the subfamily in China, belonging to *Scurrula* and *Taxillus*, respectively [9]. The genus *Scurrula* was divided into two sections: section *Cichlanthus* which includes *Scurrula pulverulenta*, *S. elata*, *S. gongshanensis*, *S. philippensis*, *S. phoebe-formosanae* and *S. notothixoides*, and section *Scurrula*, which is composed of at least five species, i.e., *S. parasitica*, *S. buddleioides*, *S. chingii*, *S. ferruginea*, and *S. sootepensis* [9]. The genus *Taxillus* was divided into three sections: section *Phyllodesmis*, which includes *Taxillus delavayi*, *T. kaempferi*, and *T. caloreas*, section *Lancilobi*, which includes *T. theifer*, *T. limprichtii*, *T. sericus*, *T. umbelifer*, *T. pseudo-chinensis*, *T. sutchuenensis*, and *T. thibetensis*, section *Spathulilibi*, which includes *T. chinensis*, *T. banlansae*, *T. nigrans*, *T. vestitus*, and *T. levinei* [9].

However, Kiu and Gilbert [8] recognized 28 species of Scurrulinae in China, including 10 species for *Scurrula* and 18 species for *Taxillus*. The authors suggested that *Scurrula* and *Taxillus* are generally similar in morphology. Nonetheless, differences in calyx and fruit shape are important to distinguish the two genera.

According to Kuijt [4], *Scurrula* comprises around 20 species distributed from India to Taiwan of China, and Malesia, while *Taxillus* includes about 30 to 35 species from South Asia, Japan, and only one species in coastal Kenya. Balle [10] initially grouped three African groups of Loranthaceae in *Taxillus* as sections *Bakerella* (Tiegh.) Balle, *Remoti* (Sprague) Balle, and *Septulina* (Tiegh.) Balle, respectively. However, they have been treated as three separate genera *Bakerella* Tiegh., *Vanwykia* Wiens, and *Septulina* Tiegh [2].

The genus *Phyllodesmis* was established by Tieghem [11] with three species *P. delavayi*, *P. paucifolia* and *P. coriacea*. However, the genus was later reduced as a section of *Taxillus* [9] or synonym of *Taxillus* [8]. The molecular phylogenetic relationships of the three genera remain unclear.

Phylogenetic studies have shown that Scurrulinae is closely related to Dendrophthoinae and African Loranthaceae [3, 5, 6, 12]. In particular, Vidal-Russell and Nickrent [3] found that Scurrulinae was the sister group of Dendrophthoinae and African Loranthaceae, but only four members of Scurrulinae were sampled.

Liu et al. [5] conducted a study on the phylogeny and historical biogeography of Loranthaceae, which included 11 samples of Scurrulinae. This study supported that Scurrulinae including *Scurrula* and *Taxillus* formed a well-supported monophyletic group, which was estimated to originate in Asia during the early Oligocene. However, the phylogeny and classification of the subtribe were not thoroughly discussed.

To resolve phylogenetic position of Scurrulinae and relationships within this group, studies with a comprehensive taxon sampling to focus on phylogenetic relationship, classification, and historical biogeography of Scurrulinae are required. The established phylogenetic framework should facilitate further collections-based integrative studies involving biogeographic and phylogenetic analyses of Scurrulinae and its close allies. Thus, the present study aims to (1) investigate phylogenetic position of the subtribe Scurrulina; (2) infer the phylogenetic relationships within Scurrulinae; and (3) establish a phylogenetically-based classification incorporating both molecular and morphological evidence.

Materials and methods

Sampling, DNA extraction, and sequencing

We collected a total of 89 individuals to ensure representation of all five tribes of the Loranthaceae, with 52 of the 89 individuals belonging to the subtribe Scurrulinae. The nuclear small-subunit ribosomal DNA (SSU rDNA), large-subunit ribosomal DNA (LSU rDNA), ribosomal internal transcribed spacer (ITS) and three plastid DNA regions (*rbcl*, *matK* and *trnL-F*) were used for analyses. Detailed voucher information and corresponding GenBank accession numbers are presented in Table S1 (Appendix).

We extracted Genomic DNA from silica gel-dried tissues by using the CTAB procedure [13]. The primers used in this study were designed by Vidal-Russell and Nickrent [3, 14], Wilson and Calvin [15] and Taberlet et al. [16] were used for PCR and sequencing (Applied Biosystems, USA). The sequences were aligned using Geneious v.8.0.5 [17].

Phylogenetic analyses

Both maximum likelihood (ML) and Bayesian inference (BI) methods were used to perform phylogenetic analyses of Scurrulinae. The GTR + I + G substitution model was determined as a best-fitting model for analysis the combined datasets of Scurrulinae by the Akaike Information Criterion (AIC) as implemented in jModelTest v.2.1.6 [18], which was accessed through the CIPRES Science Gateway [19].

The ML analysis was performed in RAxML v.8.2.12 [20, 21] with the GTR + I + G substitution model using 1000 bootstrap replicates. We conducted the Bayesian analysis in MrBayes v.3.1.2 [22] on the CIPRES Science Gateway Portal [19] applying the same substitution model as in the ML analysis. In the Bayesian analysis, the Markov chain Monte Carlo (MCMC) algorithm was set running for 10,000,000 generations with a total of four chains, starting from a random tree, and trees were sampled every 1000 generations. we checked effective sample sizes (ESSs) attained for all relevant parameters assessed (> 200) by using the program Tracer v.1.6 [23]. With the first 25% of sampled generations discarded as burn-in, the 50%

majority-rule consensus tree and Bayesian posterior probabilities (PP) were obtained using the remaining trees.

Ancestral character state reconstruction

We chose eleven morphological characters, including seven binary and four multistate ones (Table 1) for ancestral character state reconstruction. The morphological traits used to construct the character matrix were recognized by field observations, examining specimens and consulting published literature [4, 6–8, 24]. Specimens from Institute of Botany, Chinese Academy of Sciences, Beijing, China (PE), VNU University of Science, Hanoi, Vietnam (HNU) and Institute of Ecology and Biological Resources, Hanoi, Vietnam (HN) have been carefully checked in particular. Morphological characters and the coding of character states are detailed in Table S3.

Table 1

List of the 11 morphological characters and character states scored for the ancestral character state reconstruction of Scurrulinae

1.	Morphological characters and states
	Young stems tomentum: glabrous (0); hairs to glabrous (1).
2.	Leaf placement: opposite or subopposite (0); alternate (1).
3.	Leaf tomentum: glabrous (0); sparsely to densely hairy (1).
4.	Inflorescence type: umbel (0); racemes (1); subumbels (2).
5.	Corolla tomentum: glabrous (0); sparsely to densely hairy (1).
6.	Flower part number: 4 only (0); 5 only (1).
7.	Flower pedicel: absent (0); present (1).
8.	Bract: ovate to triangular (0); narrowly boat - shaped (1); ovate (2); triangular (3).
9.	Bract length: < 2 mm (0); >= 2 mm (1).
10.	Stigma: capitate (0); subcapitate (1); ovoid-subglobose (2); cone shaped (3).
11.	Fruit shape: ellipsoid or ovoid or subglobose (0); pyriform or clavate (1); cylindrical (2).

The evolutionary history of characters was reconstructed using the phylogenetic framework that included 20 species. The analysis was conducted in Mesquite v.3.61 with the “Trace Character History” option and the ML approach using the Markov k-state one-parameter (Mk1) evolutionary model [25].

Divergence time estimation

To estimate the origin and divergence times of Scurrulinae within the Loranthaceae, we used the combined datasets from nuclear (ITS, LSU rDNA and SSU rDNA) and plastid (*rbcL*, *matK*, *trnLF*) sequences for the dating analysis. This adjustment was made to match the markers used in previous phylogenetic studies from Santalales [3, 5, 6, 26].

The lineage divergence times of Scurrulinae were estimated by applying the uncorrelated lognormal Bayesian method in BEAST v.1.8.4 [27]. We partitioned the combined datasets based on six DNA regions using the “unlink substitution model” option, and on another hand, each partition was applied a substitution model from the results of jModelTest v.2.1.6 [18]. All divergence time analyses were ran using a Yule process tree prior, while, we utilized a lognormal distribution for the four calibration points. We conducted two separate MCMC runs of 150 million generations with samples taken every 1,500 generations. Tracer v.1.6 [23] was used to check whether ESSs for all relevant parameters were well above 200 and stationarity had been reached. A maximum credibility tree was then built by TreeAnnotator v.1.8.0 [28] with the initial 25% of trees discarded as burn-in. The final result was visualized in Figtree v.1.4.0 [29].

Several palaeobotanical and palynological as well as historical biogeography studies were conducted on Santalales. Most of the fossils recognized for Santalales are represented by pollen grains of Cretaceous and Tertiary periods [5, 14]. In this study, we selected one fossil calibration for the outgroups and three fossil calibrations for ingroups. The fossil pollen of *Misodendrum* (as *Compositoipollenites*) was recorded from the middle Eocene [5, 30]. The pollen record exclusively consists of dispersed pollen grains allocated to the extinct genera *Sparsipollis* and *Compositoipollenites*, which have been recognized as members of Misodendraceae [30, 31]. The fossil pollen record, although scarce, indicates that the family Misodendraceae was established in southern Patagonia by the Eocene (approximately 45 Ma) and persisted to the present [30]. Hence, the crown age of Misodendraceae was constrained to 45 Ma (95% HPD: 41.2 Ma–48.6 Ma).

For the ingroups, the stem age of Loranthaceae was constrained to 70 Ma (95% HPD: 69.4 Ma–72.6 Ma) based on the *Cranwellia* fossil [5, 31, 32]. The first occurrence of *Cranwellia* pollen was during the Campanian in Antarctica. Mildenhall [32] and Macphail et al. [31] suggested that *Cranwellia* pollen was recorded from Maastrichtian to early Pleistocene, and *Cranwellia* was assumed to be a member of Loranthaceae. We here consider that *Cranwellia* belongs to Loranthaceae, and used it to calibrate the stem node of Loranthaceae. The crown node of the tribe Lorantheae was constrained to 42.8 Ma (95% HPD: 37.8 Ma–47.8 Ma) according to the fossil pollen Changchang MT identified as *Taxillus*, *Scurrula*, and *Amyema* [26]. Changchang MT is highly similar to the pollen of Scurrulinae (*Taxillus* and *Scurrula*) and Amyeminae (*Amyema*), thus it could be an early member (probably extinct) of the Lorantheae lineage related to the core Lorantheae. Changchang MT has been used to constrain the minimum age of the MRCA of Lorantheae [5, 26] during the late Eocene. We here accept Changchang MT as Lorantheae, and used it to calibrate its crown node. The crown node of the tribe Elytrantheae was constrained to 39.6 Ma (95% HPD: 38 Ma–41.2 Ma) according to the fossil pollen Profen MT3 [26]. Profen MT3 represents some members of Elytrantheae, e.g. *Peraxilla tetrapetala* (L. f.) Tiegh., and occurred during the late Eocene [5, 26]. We thus used Profen MT3 to calibrate the crown node of Elytrantheae.

Biogeographic reconstruction

BioGeoBEARS [33] and the Bayesian approach to dispersal-vicariance analysis (Bayes-DIVA [33]) were utilized to reconstruct the biogeographic history of Scurrulinae using the time tree obtained from BEAST.

The BioGeoBEARS was conducted in R [35]. The three likelihood-based models, including Dispersal-Extinction-Cladogenesis (DEC [36]), the likelihood version of dispersal–vicariance (DIVA [37]; hereafter DIVALIKE), and the likelihood version of BayArea model [38] (hereafter BAYAREALIKE) were used to analyze the biogeographic history of Scurrulinae. In order to evaluate if descendant lineages have a different region from the direct ancestor, an additional "j" parameter (founder event/jump speciation) was added to each model [5, 33, 39]. This produced a total of six models. Additionally, using the best-fit biogeographical model and biogeographical stochastic mapping (BSM) in 'BioGeoBEARS' [40], the number and kind of biogeographical events were calculated (see the result section). According to the models, the biogeographical events were split into range expansions and founder events, vicariance, and within-area speciation events [41]. Event frequencies were estimated from the mean and standard deviation of event counts from 100 BSMs.

The Bayesian approach to dispersal-vicariance analysis was implemented in RASP v.3.2 [42, 43]. By leveraging the posterior distribution of trees produced by BEAST, the Bayes-DIVA approach can reduce phylogenetic uncertainty and produce credibility support values for alternative phylogenetic relationships [34, 42]. For the Bayes-DIVA analysis, we loaded 10,000 trees from the BEAST analysis and computed a condensed tree as the final representative tree with the first 2500 trees discarded as burn-in.

Biogeographic data for species within the subtribe Scurrulinae were compiled from the distribution information described in the literatures and herbarium specimens (PE, K, P, HN) for extant Scurrulinae and their relatives [5, 7–9]. Although the subtribe Scurrulinae is distributed in Asia and Africa, this study defined four biogeographical areas based on the distribution of extant Scurrulinae and outgroup species, considering geographic barriers and floristic divisions of Loranthaceae: A = Asia (including the mainland of South Asia, Indochina, and Malesia, but excluding New Guinea); B = Australasia (including Australia, New Zealand, New Guinea, and Pacific Islands); C = Africa (including the coastal area of the Arabian Peninsula and Sub-Saharan Africa); D = Americas (including Mexico, Central and South America). The Indian subcontinent (the mainland of South Asia) began rifting from Australia-Antarctica around 136 Ma [44], which was much earlier than the origin of the Loranthaceae and Scurrulinae [5]. Therefore, it was not defined as a separate biogeographical area. Madagascar includes only three genera of Loranthaceae, excluding Scurrulinae. Furthermore, Liu et al. [5] suggested that Madagascan Loranthaceae originated from Africa. Madagascar was thus not recognized as a biogeographical area in this study.

Results

Phylogenetic relationship

We obtained 165 sequences from 47 individuals, resulting in a matrix of 7,778 characters. Table S2 provides detailed information on each DNA region. In comparison to the combined dataset, phylogenetic trees based on distinct nuclear ribosomal and plastid partitions revealed relationships within the Scurrulinae with poorer resolution. The topologies from ML and BI analyses of the combined dataset were highly congruent and we thus present the Bayesian tree with BS and PP values in Fig. 1.

Loranthaceae was supported as monophyletic, with *Nuytsia* as sister to the remaining genera (Fig. 1). The three root parasitic genera were placed in a basal clade of Loranthaceae.

Subtribe Scurrulinae was supported as non-monophyletic. Three close genera *Phyllodesmis*, *Taxillus*, and *Scurrula* placed in three distinct subclades with strongly supported (Fig. 1). The basal subclade including only *Phyllodesmis delavayi* was well supported as sister to the remaining two genera *Taxillus* and *Scurrula*. The genus *Taxillus* was found to be closely related to *Scurrula*, and our results showed that *Taxillus* was not monophyletic with one species *Taxillus wiensii* nested in the African Loranthaceae. Within the *Taxillus* clade, *T. chinensis* was weakly supported as sister to the remaining members (BS = 70%, PP = 0.6) (Fig. 1), while the positions of *T. limprichtii* and *T. nigrans* were unresolved. *T. kaempferi*, *T. caloreas*, and *T. levinei* formed a clade with low support, and the remaining species of *Taxillus* formed a clade. Our results supported the monophyly of *Scurrula*, with *S. notothixoides* as sister to the remaining species (Fig. 1). Within the genus *Scurrula*, relationships of some species were unresolved. *S. parasitica* was a complex species that was not monophyletic and appeared in some clades within *Scurrula*. On the other hand, *Taxillus wiensii* from Africa is placed within African Loranthaceae.

Ancestral character state reconstruction

We explored the state evolution of eleven morphological characters in Scurrulinae using the combined phylogeny. Our results showed that “hairs to glabrous” young stems was the ancestral state in the subtribe, and “glabrous” was the derived state (character 1, Fig. 2A). Similarly, “sparsely to densely hairy” leaves and corollas were the ancestral states, and “glabrous” was the derived state in the subtribe (characters 3 and 5, Fig. 2B, D). The ancestral state of leaf placement was “opposite or subopposite”, and “alternate” leaf was the derived state (character 2, Fig. 2C). Our analysis revealed that “ovate” was the ancestral state of bract shape and “triangular, narrow boat-shaped, and ovate to triangular” were the derived character states (character 8, Fig. 3B). While the ancestral state of inflorescence type was unstable for the whole subtribe, our result indicated that inflorescence of *Taxillus*'s ancestor was umbel (character 4, Fig. 3A). Similarly, the ancestral state of flower part number of the subtribe was unstable (character 6, Fig. 3C). Our results showed that ancestor of *Taxillus*, *Scurrula*, and *Phyllodesmis* had 4-merous flowers (Fig. 3C). For the character 7, “flower pedicel present” was the ancestral state, and “flower pedicel absent” was the derived state (Fig. 3D), and the latter was only seen in *Taxillus wiensii*. The ancestral state of bract length (character 9) was not resolved, however, our results showed that “bract length shorter than 2 mm” was the ancestral state of *Taxillus* and *Scurrula* (Fig. 4A). Stigma “capitate” was the ancestral state, while “subcapitate”, “ovoid subglobose” and “cone-shaped” were derived (character 10, Fig. 4B). Meanwhile, fruit shape “ellipsoid or ovoid or subglobose” was found as the ancestral state, and “pyriform or clavate” and “cylindric” were derived in the subtribe (character 11, Fig. 4C).

Divergence times estimation

The divergence time estimations for the Loranthaceae and subtribe Scurrulinae are shown in Fig. 5. The crown age of Loranthaceae was estimated to be approximately 62.77 Ma (95% HPD: 53.22–75.46 Ma; node 1, Fig. 5). The tribe Lorantheae initially diverged around 42.34 Ma (95% HPD: 41.15–45.73 Ma; node 2, Fig. 5).

The subtribe Scurrulinae split from the ancestors of the subtribe Dendrophthoinae plus African Loranthaceae at 32.37 Ma (95% HPD: 26.82–37.59 Ma; node 3, Fig. 5). Within Scurrulinae, *Phyllodesmis* diverged from the remaining taxa of the subtribe at 25.46 Ma (95% HPD: 19.54–31.58 Ma; node 4, Fig. 5). The two genera *Scurrula* and *Taxillus* split from each other at 21.23 Ma (95% HPD: 15.77–27.27 Ma; node 6, Fig. 5), then started to diversify at 16.73 Ma (95% HPD: 11.33–22.73 Ma; node 7, Fig. 5) and 16.30 Ma (95% HPD: 10.70–22.39 Ma; node 8, Fig. 5), respectively. Additionally, *Taxillus wiensii* separated with *Oedina pendens* at 17.78 Ma (95% HPD: 8.84–25.98 Ma; node 5, Fig. 5).

Ancestral area reconstruction

Our ancestral area reconstruction using BioGeoBEARS and Bayes-DIVA yielded highly congruent results. Among the six models used in our BioGeoBEARS analysis, models including three parameters had higher log likelihood values than models including two parameters (Table 2), indicating jump speciation (i.e., dispersal between non-adjacent areas) as an important pattern in range variation of Loranthaceae. Moreover, the BioGeoBEARS analyses showed DEC + j as the best-fit biogeographic model. Therefore, we present only the reconstruction of BioGeoBEARS under the DEC + j model (Fig. 6). Additionally, the result of ancestral area reconstructions from Bayes-DIVA is shown in Fig. S1. Node numbers in Figs. 5 and 6 are consistent, and we summarize the divergence time estimations and ancestral area reconstruction in Table 3. Biogeographic stochastic mapping (BSM) under the DEC + j model indicated that most biogeographic events comprised within-area speciation (78%) and dispersals (20.7%), with very few (1.3%) vicariant events (Table S4). The stem group of Scurrulinae was estimated to originate from Asia (area A) (node 3, Fig. 6), and Scurrulinae subsequently diversified in Asia during the Oligocene. The genus *Phyllodesmis* was estimated to originate in Asia during the Late Oligocene (node 4, Fig. 6). *Taxillus* and *Scurrula* also originated in Asia and diversified during the middle Miocene (nodes 7 and 8, Fig. 6). Additionally, the only African member of Scurrulinae (*Taxillus wiensii*) was estimated to diverge from its African relative during the Miocene (nodes 5, Fig. 6).

Table 2

Comparison of the fit of different models of biogeographic range evolution and model specific estimates for different parameters (d = dispersal, e = extinction, j = weight of jump dispersal (founder speciation)).

Model	Parameter No	LnL	d	e	j	AIC	AIC weight
DEC	2	-48.79	4.5×10^{-4}	0.3161	0	102.70	0.0398
DEC + j	3	-48.35	2.4×10^{-4}	0.3255	0.0169	96.33	0.960
DIVALIKE	2	-49.60	4.0×10^{-4}	0.1499	0	105.90	0.013
DIVALIKE + j	3	-51.96	3.3×10^{-5}	1.0×10^{-12}	0.0186	97.20	0.99
BAYAREALIKE	2	-62.40	5.5×10^{-5}	0.0168	0	115.45	1
BAYAREALIKE + j	3	-49.12	1.2×10^{-4}	0.0058	0.0215	109.23	0.65

Table 3

Summary of supported clades, divergence age estimation (Ma) by BEAST and ancestral area reconstructions by Bayes-DIVA and maximum likelihood. Node numbers refer to Figs. 5, 6. Area abbreviations are as follows: A = Asia (including mainland of South Asia, Indochina and Malesia, but excluding New Guinea); B = Australasia (including Australia, New Zealand, New Guinea, and Pacific Islands); C = Africa (including the coastal area of the Arabian Peninsula and Sub-Saharan Africa); D = Americas (including Mexico, Central and South America).

Node	Bayesian PP	Age estimates mean (95% HPD) [Ma]	BioGeoBEARS (DEC + j)	Likelihood-DEC (relative probability)	Bayes-DIVA (maximum probability)
1	1.0	59.38 (52.58, 65.59)	A	A A (0.94)	A (94.64)
2	1.0	51.30 (45.71, 57.42)	C	C C (0.95)	C (97.22)
3	1.0	50.04 (44.61, 55.90)	A	A A (0.94)	A (86.93)
4	1.0	48.05 (42.39, 53.15)	A	A A (0.94)	A (75.52)
5	< 0.90	39.33 (36.48, 42.12)	A	A A (0.94)	A (65)

Discussion

Phylogenetic relationship

With extensive taxon and gene sampling, this study retrieves a well-supported topology for most clades, although some subclades within the genera *Taxillus* and *Scurrula* exhibit weak support (Fig. 1). Our results demonstrate that the subtribe Scurrulinae is non-monophyletic, with one species, *Taxillus wiensii*, nested within the African Loranthaceae clade. *Phyllodesmis* is strongly supported as sister to the two genera, *Taxillus* and *Scurrula*. Morphological characters are useful to support relationships within the subtribe, particularly the glabrous young stems and leaves can distinguish *Phyllodesmis* from *Taxillus* and *Scurrula* (Fig. 2A, B). *Taxillus wiensii* clade characterized by bract shape, flower part number, flower pedicel (Fig. 3B, C, D), while, the clade of *Taxillus* and *Scurrula* characterized by bract length (Fig. 4A). Our character optimizations suggest that the two genera *Taxillus* and *Scurrula* are very similar in morphology, and they share ancestral morphological states of most characters. However, they have evolved differently in the shape of fruit and stigma (Fig. 4B, C). Based on our observation of specimens and fresh plants in the field, fruits of *Scurrula* are always pyriform or clavate sometimes, while those of *Taxillus* are usually ellipsoid, ovoid, or cylindrical.

Scurrula comprises around 50 species in China and Southeast Asia. Our phylogenetic analysis revealed unexpected relationships between the *S. parasitica* complex and the *S. chingii* complex (Fig. 1). *S. parasitica* was found to be a complex member in this study based on molecular data, with two varieties: *S. parasitica* var. *parasitica* and *S. parasitica* var. *graciliflora*. Our results demonstrated that *S. parasitica* var. *parasitica* and *S. parasitica* var. *graciliflora* are not monophyletic (Fig. 1). Moreover, *S. parasitica* var. *graciliflora* is distantly from *S. parasitica* in the molecular phylogenetic tree (Fig. 1), which can be easily distinguished from *S. parasitica* var. *parasitica* by its greenish-yellow corolla (versus red corolla in *S. parasitica* var. *parasitica*). Based on our findings, we suggest that *S. parasitica* var. *graciliflora* should be redefined as a separate species. A detailed treatment of this taxon will be provided in a future study.

Scurrula chingii is composed of two varieties: *S. chingii* var. *yunnanensis* and *S. chingii* var. *chingii* [8]. Both varieties are non-monophyletic by Liu et al. [5] and our study (Fig. 1). Although the position of *S. chingii* var. *yunnanensis* is uncertain in our phylogenetic tree, it is distant from *S. chingii* var. *chingii* as reported by Liu et al. [5]. Furthermore, *S. chingii* var. *yunnanensis* can be easily distinguished from *S. chingii* var. *chingii* based on several characteristics, including glabrous leaf blade surfaces (versus rusty red tomentose or glabrous abaxial surface in *S. chingii* var. *chingii*), shorter peduncle and floral axis less than 10 mm (vs. 10–25 mm in *S. chingii* var. *chingii*), and lanceolate corolla lobes (versus subspatulate lobes in *S. chingii* var. *chingii*). Additionally, *Scurrula chingii* var. *yunnanensis* is endemic to Yunnan (China), while *S. chingii* var. *chingii* is distributed in Guangxi, southern Yunnan (China), and northern Vietnam. Based on our results, *S. chingii* var. *yunnanensis* should be redefined to the species rank. The detail treatment will be provided in a future study.

Taxillus includes approximately 35 species from tropical Asia (India and Sri Lanka to China, Japan, Philippines, Borneo) and Africa (Kenya coast). *Taxillus* is generally characterized by low host specificity. *Taxillus chinensis* (DC.) Danser, a Malesian species, is widely distributed in west of Charles's Line. On the other hand, *T. wiensii* Polhill, the only species of *Taxillus* in East Africa, has a narrow distribution limited to the Kenya coast.

Polhill and Wiens [7] suggested that although the morphology of *T. wiensii* is similar to the species of *Taxillus* in Sri Lanka, the flowers of *T. wiensii* appear different from the Asiatic species due to the erect and possibly spontaneously open corolla-lobes. Additionally, Polhill and Wiens [7] proposed that *T. wiensii* is more comparable to the African genera that have been segregated from sections of *Taxillus* based on flower characteristics, such as sect. *Bakerella* (Tieghem) Balle, sect. *Remoti*, and sect. *Septulina*. Furthermore, all species of Loranthaceae in continental Africa and Madagascar, except *Socratina* and one species of *Septulina*, can be distinguished by their flowers that open spontaneously with erect or spreading corolla-lobes, rather than explosively as in *Taxillus*. *Bakerella* is entirely glabrous, while *Socratina* is hairy, with a unique occurrence of fine indumentum on the inner face of the corolla-lobes. In terms of morphology, *T. wiensii* can be distinguished from the Asian *Taxillus* by its 5-merous (rather than 4 merous) flowers and bract shape (as shown in Fig. 3C). Our analyses of character optimizations indicate that *T. wiensii* and the Asian *Taxillus* have evolved differently in terms of flower and bract structure. It is difficult to improve the generic classification without detailed consideration of relationship between *T. wiensii* and the Asian *Taxillus* species [7]. Our molecular results indicate that *T. wiensii* is placed within African Loranthaceae and is clearly different from the Asian *Taxillus* (Fig. 1). Therefore, we strongly suggest that the African *Taxillus* should be recognized as a new genus, and we propose the name *Afrotaxillus* for this taxon.

Furthermore, our molecular analyses revealed that *Taxillus limprichtii* and its variety *T. limprichtii* var. *longiflorus* (Lecomte) H. S. Kiu do not form a monophyletic group. Therefore, we recommend that their taxonomic classification be reevaluated in future studies.

Phyllodesmis, comprised four species, was initially described by Tieghem [11]. However, subsequent research reduced this genus to a synonym of *Taxillus*, incorporating *T. delavayi* (Tieghem) Danser, *T. kaempferi* (Candolle) Danser, *T. caloreas* (Diels) Danser, and *T. renii* H.S. Kiu [8]. Our results support *Phyllodesmis* as a distinct clade from *Taxillus* and *Scurrula* with strong support (Fig. 1). Moreover, the *Phyllodesmis* clade includes only *P. delavayi*, a species that does not parasitize species of Pinaceae, unlike the remaining three species. Furthermore, *Phyllodesmis* can be easily distinguished from all other *Taxillus* members based on characteristics of leaves alternate (as apposed to opposite or subopposite), glabrous young branchlets (not densely stellately hairy), and both surfaces of leaves glabrous (not hairy on at least one surface) (Fig. 7). Thus, we suggest reinstating *Phyllodesmis* as a recognized genus, comprising only one species, *P. delavayi*.

Taxonomic treatment of *Phyllodesmis*

Phyllodesmis Tiegh. in Bull. Soc. Bot. France 42: 255. 1895 (Fig. 7)

Aerial parasite, small shrubs, glabrous. Leaves alternate, sometimes subopposite, pinnately veined. Inflorescences at leafless node, umbels 2–4-flowered; 1 bract subtending each flower, usually scale-like. Flowers bisexual, 4-merous, zygomorphic. Calyx ellipsoid or ovoid, rarely subglobose, base not attenuate, limb annular, entire or denticulate, persistent. Mature flower bud tubular, tip ellipsoid. Corolla sympetalous, slightly curved, basal portion ± inflated, split along 1 side at anthesis, lobes all reflexed toward the side away from the split, red, glabrous. Stamens inserted at base of corolla lobes; filaments short; anthers 4-loculed. Pollen grain trilobate or semilobate in polar view. Ovary 1-loculed; placentation basal. Style filiform, 4-angled; stigma usually capitate. Berry ellipsoid or ovoid, exocarp leathery, verrucose or granular, rarely smooth, pubescent or glabrous, base rounded.

Phyllodesmis delavayi Tieghem, Bull. Soc. Bot. France 42: 255. 1895. *Taxillus delavayi* (Tieghem) Danser, Verh. Kon. Ned. Akad. Wetensch., Afd. Natuurk., 29(6): 123. 1933. Type: China, Yunnan, Dali, Feb. 1887, *Delavay 2620* (P!).

Morphology

—Aerial parasite, small shrubs ca. 0.5-1 m tall, glabrous. Branches gray-brown to blackish, often very minutely transversely wrinkled, young branchlets glabrous. Leaves alternate, sometimes subopposite, petiole 2–4 mm; leaf blade ovate, or elliptic to lanceolate, 3–6 × 1.3–2.5 cm, leathery, both surfaces glabrous, lateral veins 3 or 4 pairs, base cuneate, slightly decurrent, apex obtuse, adaxial surface of young leaf brown, especial leaf edge; abaxial surface green. Umbels solitary or 2 together, sometimes at leafless node, 2-7-flowered; peduncle 0–2 mm; bracts ovate, ca. 2 mm, glabrous, rarely long bearded at tip. Pedicel 5–15 mm. Calyx ellipsoid, ca. 2.5 mm, limb annular, entire or minutely 4-toothed. Mature bud 4–5 cm, tip ellipsoid, tip inside yellow. Corolla red, slightly curved, glabrous, lobes lanceolate, 3–9 mm, reflexed. Filaments short ca. 2 mm; anthers 1.5 mm. Ovary 1-loculed; placentation basal. Stigma capitate. Berry yellow or orange, ellipsoid, 8–10 × 3–4 mm, glabrous.

Phenology

—Flowering in Feb–May, fruiting in Apr–Sep.

Habitat

—Forests, mountain slopes; 1500–3000 m.

Conservation

—While not threatened as a species, and not listed under IUCN criteria, some populations of *Phyllodesmis* do require protection from over collection for medicinal use.

Distribution:—China: Yunnan, Guangxi, Sichuan, Xizang; Myanmar, and Vietnam: Lao Cai, Lai Chau.

Selected specimens examined:—VIETNAM: Lao Cai: Sapa district, San Sa Ho commune, Cat Cat village, October 2019, Van Du Nguyen, Hung Manh Nguyen, Xuan Thanh Trinh and Chi Toan Le DMTT38, DMTT39 (HN). CHINA: Sichuan: Dêrong County, Zigen, Jul 1981, *Qinghai-Tibetan Expedition Team 1734* (PE); Shimian County, 1955, *C.J. Xie 39892* (PE). Xizang: Zayü County, Shangchayu, Jul 1980, *C.C. Ni et al. 740* (PE). Yunnan: Wenshan County, Mt. Laojun, April 1993, *Y.M. Shui 1904* (PE); Dêqên County, Benzilan, July 1981, *Qinghai-Tibetan Expedition Team 1864* (PE).

Historical biogeography of Scurrulinae

Asian origin of Scurrulinae

Our divergence time estimations for Scurrulinae are consistent with those from Magallón et al. [45], Grímsson et al. [26], and Liu et al. [5] (Table S5). The biogeographic analyses and divergence time estimations suggest that the stem group of Scurrulinae originated in Asia ca. 32.37 Ma during the Oligocene (node 3, Figs. 5, 6; Table 3), with a crown age dating back to 25.46 Ma (95% HPD: 19.54–31.58 Ma; node 4, Figs. 5, 6; Table 3). The Indian subcontinent began rifting from Australia-Antarctica ca. 136 Ma [44], and connected to mainland Asia ca. 44 Ma. Thus, the connection between India and Asia occurred much earlier than the origin of the Scurrulinae. According to Li et al. [46], the uplift of high mountains in Asia during the Oligocene-Miocene, combined with the southwest monsoon in Asia, probably provided ideal conditions for colonization and wide distribution of Scurrulinae. Additionally, short-distance dispersal in Asia is also important for domination or wide distribution of plants. Therefore, Asian Scurrulinae, including Indian Scurrulinae, likely originated in Asia and may have spread throughout the area by birds or small animals [47–49].

Our study confirms the findings of Liu et al. [5] that Asian Loranthaceae migrated from Australia in the late Eocene. Notably, despite several species of Scurrulinae being found in Malaysia, Indonesia, and the Philippines [4, 8, 9], which are geographically close to Australasia, there is no evidence of Scurrulinae dispersing from Asia to Australasia. While several Loranthaceae genera are common to both regions, including *Lepeostegeres*, *Amylotheca*, *Decaisnina*, *Macrosolen*, and *Cecarria* [5], our study, along with Liu et al. [5] suggests that all migration events from Asia to Australasia occurred before about 35 Ma, which is earlier than the origin of Scurrulinae. Thus, the *Phyllodesmis*, *Taxillus* and *Scurrula* of Scurrulinae may be endemic genera to Asia.

Liu et al. [5] proposed that within-area speciation events are more prevalent in most of the large clades that are endemic to single areas of Loranthaceae. They suggested that dispersal without “range contractions” was the main driver of range evolution, occurring more frequently than vicariance events. Our BSM results (Table S4) are consistent with Liu et al. [5] that within-area speciation events are the main factor in creating the Asian endemic group of Scurrulinae. Dispersal events have been considered as the most common factor for worldwide distributed plants, including Loranthaceae and Scurrulinae lineages [5, 41]. Our BSM indicates that the dispersal events of Scurrulinae occurred without “range contractions” or “founder events”, which is consistent with biogeographic history of the subtribe Scurrulinae (Fig. 6). After originating in Asia, Scurrulinae did not disperse to other regions. African

Loranthaceae evolved from an Asian ancestor [5], and *Taxillus wiensii* originated in Africa from the African Loranthaceae ancestor. Short-distance dispersal events between proximal regions appear to have been frequent in the historical biogeography of Scurrulinae, and it may have been facilitated by the colonization or domination of Scurrulinae host plants in tropical forests.

Species of Loranthaceae are distributed worldwide [2, 4, 5, 8]. However, due to geographic distance, climate change, and special evolutionary direction, they are becoming endemic groups for each continent, resulting in fewer shared genera. Our results suggest that Scurrulinae originated and diverged in Asia during a period when rainforests dominated the continent [50] (Fig. 6). The members of this subtribe evolved and adapted to the living conditions in Asia, and the rapid climate changes, cooling, drying, and the progressive uplift of the high mountains in central Asia, especially during the late Pliocene and Pleistocene, might have promoted the diversification of Scurrulinae and prevented their dispersal to other continents. Our study does not recognize any migration of Scurrulinae to other continents since the early Oligocene, except for one species of *Taxillus* that originated in Africa.

African origin and diversification of "Afrotaxillus"

The present study supports that the placement of "*Afrotaxillus wiensii*" (*Taxillus wiensii*) within Africa Loranthaceae and its close relationship to *Tapinanthus constrictiflorus* (Figs. 1, 6). Biogeographic analyses indicate that "*Afrotaxillus*" originated and diversified in Africa (Fig. 6), and this genus is likely not part of Scurrulinae. *Taxillus wiensii*, formerly known as "*Afrotaxillus wiensii*" was considered as the only member of *Taxillus* in Africa, with dispersal from Asia to Africa proposed to explain its historical biogeography [5, 7]. However, this study confirms that the ancestor of "*Afrotaxillus*" is African Loranthaceae, and this genus likely evolved separately from *Taxillus* in Asia ca. 17 Ma (Figs. 5, 6). A similar situation was encountered in the genus *Helixanthera*, with Liu et al. [5] demonstrating differences between African and Asian *Helixanthera* and suggesting that African *Helixanthera* may be recognized as a distinct genus in the future studies.

Conclusion

Based on comprehensive taxon sampling of the subtribe Scurrulinae, this study strongly supports the relationship among genera of the subtribe. *Phyllodesmis* is recognized as a separate genus from its allies *Taxillus* and *Scurrula* while "*Afrotaxillus*" is confirmed as a new genus from Africa. The mistletoe Scurrulinae originated in Asia during the Oligocene, and then was widespread in Asia and did not disperse to other areas. *Taxillus* and *Scurrula* diverged during the climatic optimum in the middle Miocene. "*Afrotaxillus*" originated in Africa from African Loranthaceae approximately 17 Ma, clearly different from *Taxillus* in Asia. Diversification of Scurrulinae and the development of endemic species in Asia may have been promoted by the fast-changing climate, including cooling, drying, and the progressive uplift of the high mountains in central Asia, especially during the late Pliocene and Pleistocene.

Declarations

Acknowledgements

Not applicable.

Authors' contributions

BL and CTL conceived and designed the experiment. CTL and WOO performed the experiments. LML, ZDC, VDN and CTL assisted in data analysis. CTL and BL wrote the manuscript. All the authors read and approved the final version of the manuscript.

Funding

This research is funded by National Natural Science Foundation of China (31970212 and 31800178), the National Key Research Development Program of China (2022YFF0802300, 2022YFC2601200), the International Partnership Program of CAS (151853KYSB20190027), Sino-Africa Joint Research Centre, Chinese Academy of Sciences, CAS International Research and Education Development Program (SAJC202101), and Vietnam National Foundation for Science and Technology Development (NAFOSTED) under grant No. 106.03-2019.12.

Availability of data

All data and plant material used to draw conclusions presented in this manuscript is shown in Table 1 and can be provided based upon reasonable request to the corresponding author.

Ethics approval and consent to participate

All methods were in accordance with relevant institutional, national, and international guidelines and legislation.

Consent for publication

Not applicable.

Competing interests

The authors declare no competing interests.

References

1. Nickrent DL. The parasitic plant connection. 2017. Available at: <http://parasiticplants.siu.edu/>. Last accessed September 6, 2017.
2. Nickrent DL, Malécot V, Vidal-Russell R, Der JP. A revised classification of Santalales. *Taxon*. 2010;59:538–58.

3. Vidal-Russell R, Nickrent DL. Evolutionary relationship in the showy mistletoe family (Loranthaceae). *Am J Bot.* 2008a;95:1015–29.
4. Kuijt J. Santalales. In: Kubitzki K, editor. *The families and genera of vascular plants, Flowering plants: Eudicots; Santalales, Balanophorales.* Volume 12. Cham, Switzerland: Springer; 2015. pp. 2–189.
5. Liu B, Le CT, Barrett RL, Nickrent DL, Chen ZD, Lu LM, Vidal-Russell R. Historical biogeography of Loranthaceae (Santalales): diversification agrees with emergence of tropical forests and radiation of songbirds. *Mol Phylogenet Evol.* 2018;124:199–212.
6. Su HJ, Hu JM, Anderson FE, Der JP, Nickrent DL. Phylogenetic relationships of Santalales with insights into the origins of holoparasitic Balanophoraceae. *Taxon.* 2015;64:491–506.
7. Polhill R, Wiens D. *Mistletoes of Africa.* Richmond-Surrey, UK: The Royal Botanic Gardens Kew; 1998.
8. Kiu HS, Gilbert MG. Loranthaceae. In: Wu ZY, Raven PH, Hong DY, editors. *Flora of China.* Volume 5. Beijing, China: Science Press; St. Louis, USA: Missouri Botanical Garden Press;; 2003. pp. 220–39.
9. Kiu HS. Loranthaceae. In: Kiu HS, Ling YR, editors. *Flora Reipublicae Popularis Sinicae.* Volume 24. Science Press, Beijing;; 1988. pp. 86–158. [In Chinese.].
10. Balle S. A propos de la morphologie des "*Loranthus*. d'Afrique Webbia. 1955;11:541–85.
11. Tieghem PV. *Taxillus.* *Bull Bot Soc France.* 1895;42: 255.
12. Vidal-Russell R, Nickrent DL. The biogeographic history of Loranthaceae. *Darwiniana.* 2007;45:34–54.
13. Doyle JJ, Doyle JL. A rapid DNA isolation procedure for small quantities of fresh leaf tissue. *Phytochem Lett.* 1987;19:11–5.
14. Vidal-Russell R, Nickrent DL. The first mistletoes, origins of aerial parasitism in Santalales. *Mol Phylogenet Evol.* 2008b;47:523–37.
15. Wilson CA, Calvin CL. An origin of aerial branch parasitism in the mistletoe family, Loranthaceae. *Am J Bot.* 2006;93:787–96.
16. Taberlet P, Gielly L, Pautou G, Bouvet J. Universal primers for amplification of three non-coding regions of chloroplast DNA. *Plant Mol Biol.* 1991;17:1105–9.
17. Kearse M, Moir R, Wilson A, Stones-Havas S, Cheung M, Sturrock S, Buxton S, Cooper A, Markowitz S, Duran C, Thierer T, Ashton B, Meintjes P, Drummond A. Geneious basic: an integrated and extendable desktop software platform for the organization and analysis of sequence data. *Bioinformatics.* 2012;28:1647–9.
18. Darriba D, Taboada GL, Doallo R, Posada D. JModelTest 2: more models, new heuristics and high-performance computing. *Nat Methods.* 2012;9:772.
19. Miller MA, Pfeiffer W, Schwartz T. Creating the CIPRES Science Gateway for inference of large phylogenetic trees. In: *Proceedings of the Gateway Computing Environments Workshop (GCE).* Institute of Electrical and Electronics Engineers (IEEE), New Orleans, USA, 2010; 1–8.

20. Stamatakis A. RAxML-VI-HPC, maximum likelihood-based phylogenetic analyses with thousands of taxa and mixed models. *Bioinformatics*. 2006;22:2688–90.
21. Stamatakis A, Hoover P, Rougemont J. A rapid bootstrap algorithm for the RAxML Web servers. *Syst Biol*. 2008;57:758–71.
22. Ronquist F, Huelsenbeck JP. MrBayes 3: Bayesian phylogenetic inference under mixed models. *Bioinformatics*. 2003;19:1572–4.
23. Rambaut A, Suchard MA, Xie D, Drummond AJ. Tracer v1.6. 2014. Available at <http://tree.bio.ed.ac.uk/software/tracer/>.
24. Su HJ, Liang SL, Nickrent DL. Plastome variation and phylogeny of *Taxillus* (Loranthaceae). *PLoS ONE*. 2021;16(8):e0256345.
25. Maddison WP, Maddison DR. Mesquite: a modular system for evolutionary analysis. 2019. Version 3.61. <http://www.mesquiteproject.org>.
26. Grímsson F, Kapli P, Hofmann CC, Zetter R, Grimm GW. Eocene Loranthaceae pollen pushes back divergence ages for major splits in the family. *PeerJ*. 2017;5:e3373.
27. Drummond AJ, Suchard MA, Xie D, Rambaut A. Bayesian phylogenetics with BEAUti and the BEAST 1.7. *Mol Biol Evol*. 2012;29:1969–73.
28. Rambaut A, Drummond AJ. TreeAnnotator. Version 1.8, distributed as part of the BEAST Package. 2010. Available at: <http://beast.community/installing>.
29. Rambaut A. FigTree v.1.4. 2009. Available at: <http://tree.bio.ed.ac.uk/software/figtree/>.
30. Zamaló MDC, Fernández CA. Pollen morphology and fossil record of the feathery mistletoe family Misodendraceae. *Grana*. 2016;55:278–85.
31. Macphail M, Jordan G, Hopf F, Colhoun E. When did the mistletoe family Loranthaceae become extinct in Tasmania? Review and conjecture. In: Haberle SG, David B, editors. *Peopled landscapes (Terra Australis 34) archaeological and biogeographic approaches to landscapes*. Canberra: Australian National University; 2012. pp. 255–70.
32. Mildenhall DC. New Zealand Late Cretaceous and Cenozoic plant biogeography: a contribution. *Palaeogeogr Palaeoclimatol Palaeoecol*. 1980;31:197–233.
33. Matzke NJ. Probabilistic historical biogeography: new models for founderevent speciation, imperfect detection, and fossils allow improved accuracy and model-testing. *Front Biogeogr*. 2013;5:242–8.
34. Nylander JA, Olsson U, Alstrom P, Sanmartin I. Accounting for phylogenetic uncertainty in biogeography: a Bayesian approach to dispersal vicariance analysis of the thrushes (Aves: *Turdus*). *Syst Biol*. 2008;57:257–68.
35. R Core Team. R: A language and environment for statistical computing. R foundation for statistical computing. Austria: Vienna; 2016.
36. Ree RH, Smith SA. Maximum likelihood inference of geographic range evolution by dispersal, local extinction, and cladogenesis. *Syst Biol*. 2008;57:4–14.

37. Ronquist F. Dispersal-vicariance analysis: a new approach to the quantification of historical biogeography. *Syst Biol.* 1997;46:195–203.
38. Landis MJ, Matzke NJ, Moore BR, Huelsenbeck JP. Bayesian analysis of biogeography when the number of areas is large. *Syst Biol.* 2013;62:789–804.
39. Lian L, Xiang KL, Ortiz RDC, Wang W. A multi-locus phylogeny for the Neotropical Anomospermeae (Menispermaceae): Implications for taxonomy and biogeography. *Mol Phylogenet Evol.* 2019;136:44–52.
40. Matzke NJ. Stochastic mapping under biogeographical models. 2015. Available at: http://phylo.wikidot.com/biogeobears#stochastic_mapping (accessed 1 June 2015).
41. Dupin J, Matzke NJ, Särkinen T, Knapp S, Olmstead RG, Bohs L, Smith SD. Bayesian estimation of the global biogeographical history of the Solanaceae. *J Biogeogr.* 2017;44:887–99.
42. Yu Y, Harris AJ, He X. RASP (Reconstruct Ancestral State in Phylogenies) 2.0 Beta. 2011. Available at: <http://mnh.scu.edu.cn/soft/blog/RASP>.
43. Yu Y, Harris AJ, Blair C, He X. RASP (Reconstruct Ancestral State in Phylogenies): A tool for historical biogeography. *Mol Phylogenet Evol.* 2015;87:46–9.
44. Gibbons AD, Whittaker JM, Müller RD. The breakup of East Gondwana: Assimilating constraints from Cretaceous ocean basins around India into a best-fit tectonic model. *J Geophys Res.* 2013;118:808–22.
45. Magallón S, Gómez-Acevedo S, Sánchez-Reyes LL, Hernández-Hernández T. A metacalibrated time-tree documents the early rise of flowering plant phylogenetic diversity. *New Phytol.* 2015;207:437–53.
46. Li M, Tetsuo OT, Gao YD, Xu B, Zhu ZM, Ju WB, Gao XF. Molecular phylogenetics and historical biogeography of *Sorbus* sensu stricto (Rosaceae). *Mol Phylogenet Evol.* 2017;111:76–86.
47. Amico G, Aizen MA. Mistletoe seed dispersal by a marsupial. *Nature.* 2000;408:929–30.
48. Klicka J, Voelker G, Spellman GM. A molecular phylogenetic analysis of the “true thrushes” (Aves: Turdinae). *Mol Phylogenet Evol.* 2005;34:486–500.
49. Cibois A, Thibault JC, Bonillo C, Filard CE, Watling D, Pasquet E. Phylogeny and biogeography of the fruit doves (Aves: Columbidae). *Mol Phylogenet Evol.* 2013;70:442–53.
50. Weeks A, Daly DC, Simpson BB. The phylogenetic history and biogeography of the frankincense and myrrh family (Burseraceae) based on nuclear and chloroplast sequence data. *Mol Phylogenet Evol.* 2005;35:85–101.

Figures

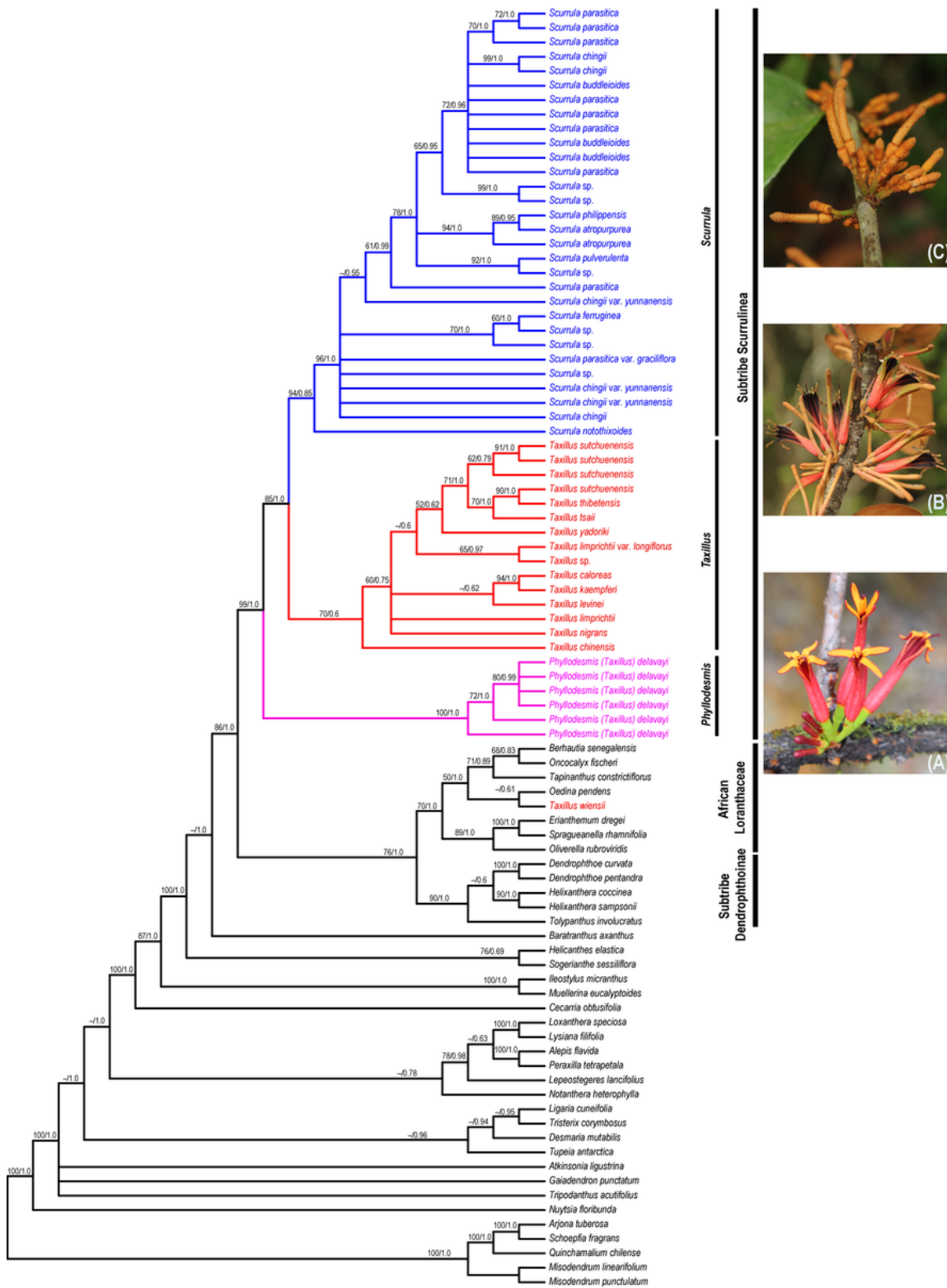


Figure 1

Majority rule consensus tree of Scurrulinae based on Bayesian inference of the combined dataset of six DNA regions (LSU rDNA, SSU rDNA, ITS, *matK*, *rbcl* and *trnL-F*). ML bootstrap values and posterior probabilities (PP) of the BI analysis are presented above the branches. “-” indicates the support values less than 50%. **(A)**. *Phyllodesmis delavayi*; **(B)**. *Taxillus thibetensis*; **(C)**. *Scurrula yunnanensis*. Photo credits: C. T. Le (A, B). Liu (B, C).

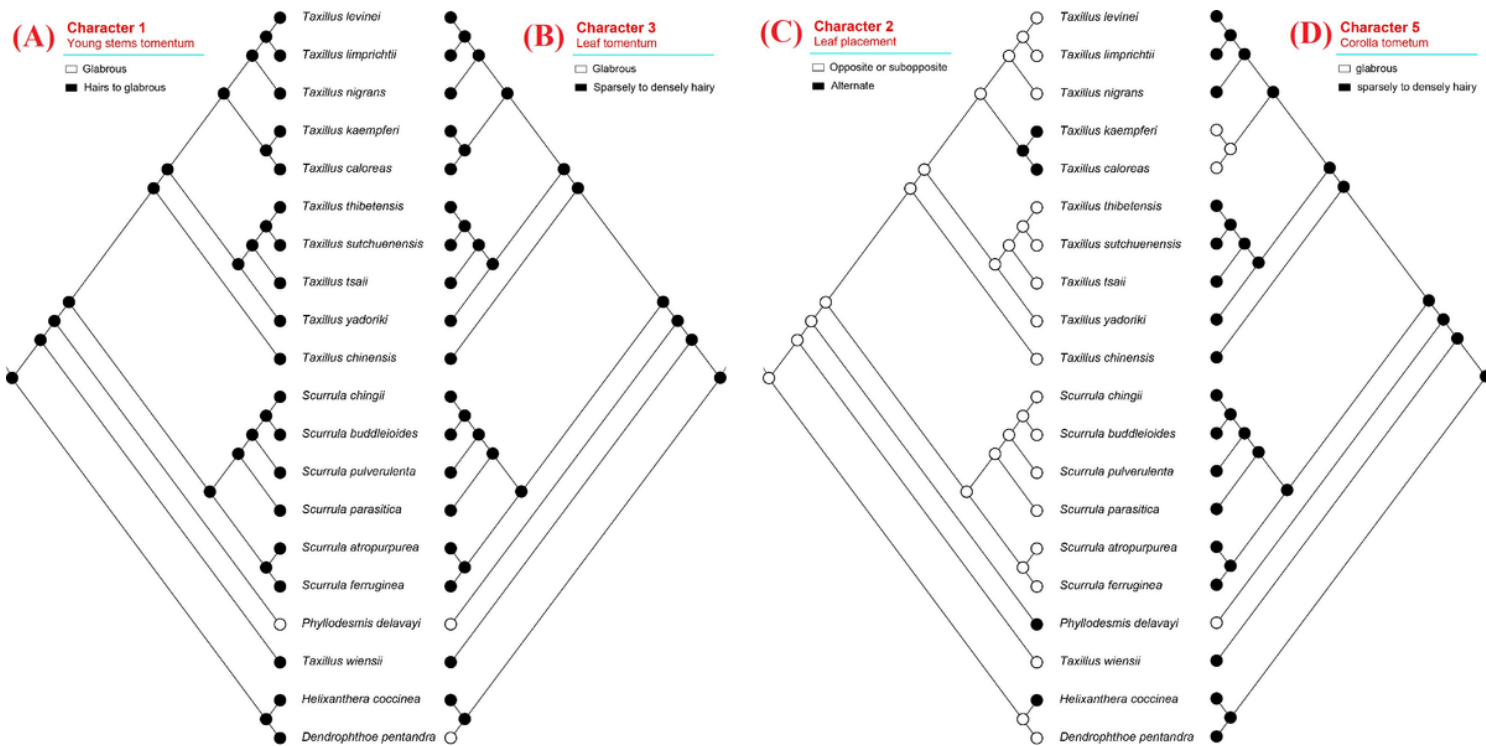


Figure 2

Character optimization of four morphological characters using the molecular phylogeny. A. Young stems tomentum; B. leaf tomentum; C. leaf placement; D. corolla tomentum.

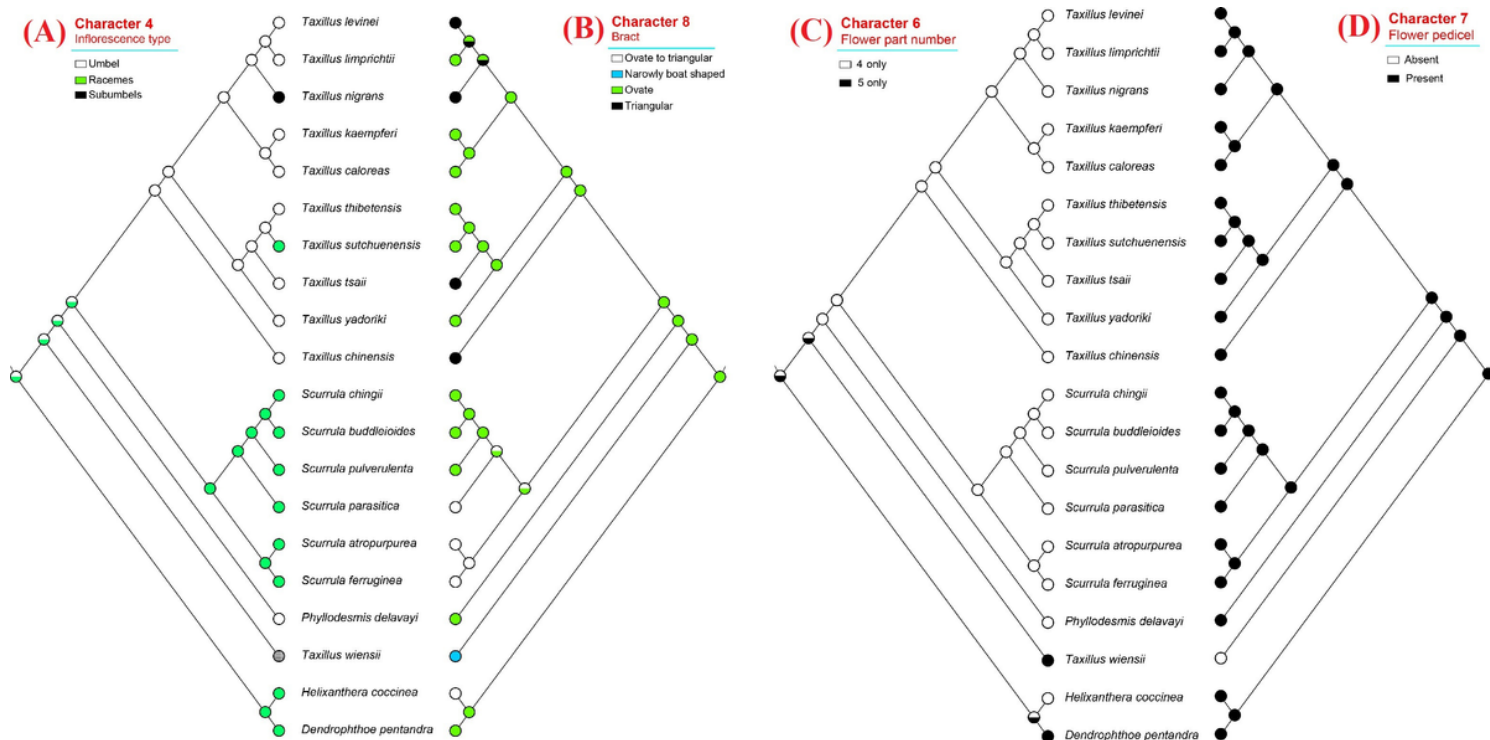


Figure 3

Character optimization of four morphological characters using the molecular phylogeny. A. Inflorescence type; B. bract; C. flower part number; D. flower pedicel.



Figure 4

Character optimization of three morphological characters using the molecular phylogeny. A. Bract length; B. stigma; C. fruit shape.

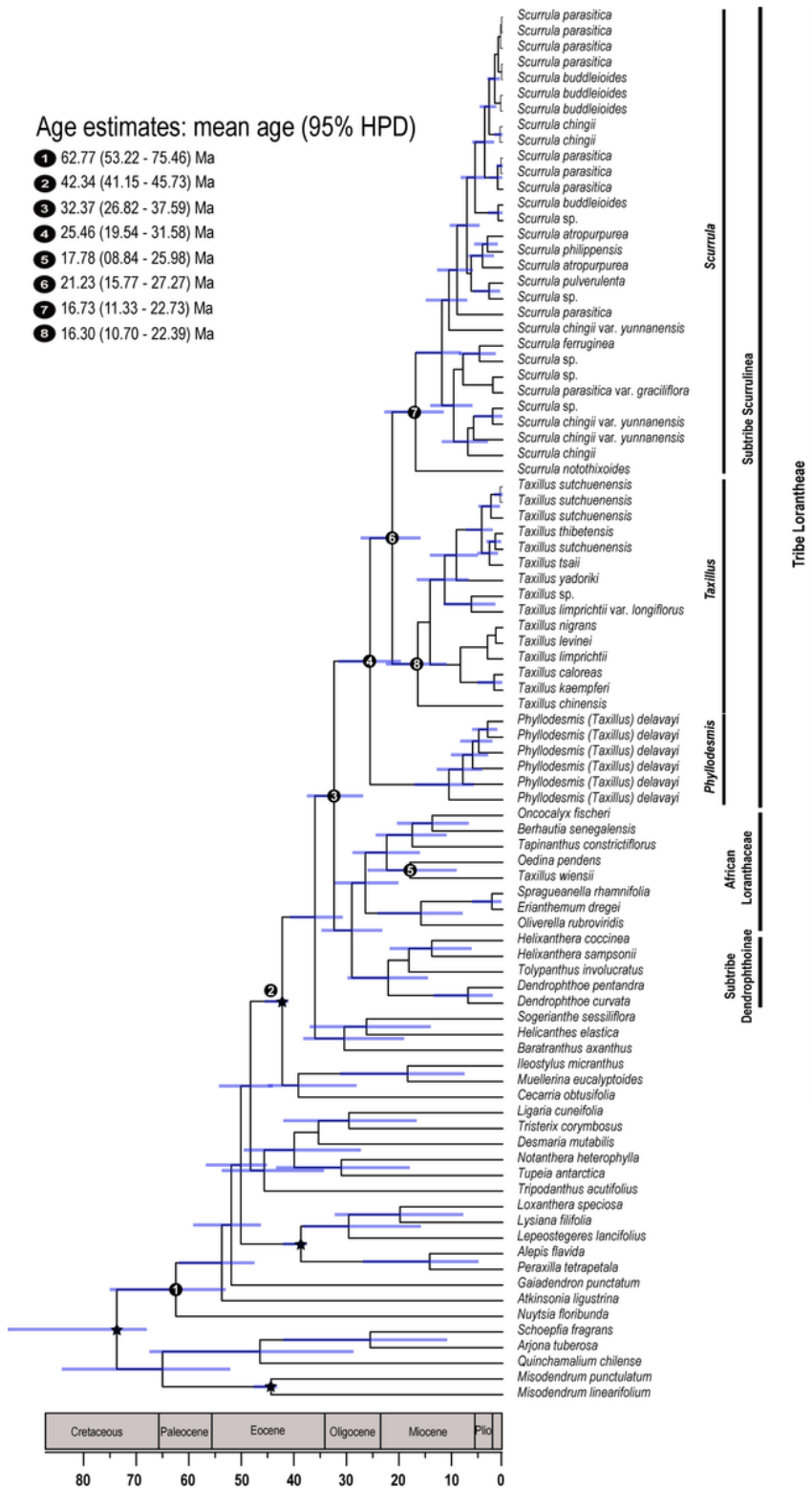


Figure 5

Maximum clade credibility tree inferred from BEAST based on the combined datasets of six DNA regions. The bars around node ages indicate 95% highest posterior density intervals. Node constraints are indicated with stars. Nodes of interests were marked as 1–6.

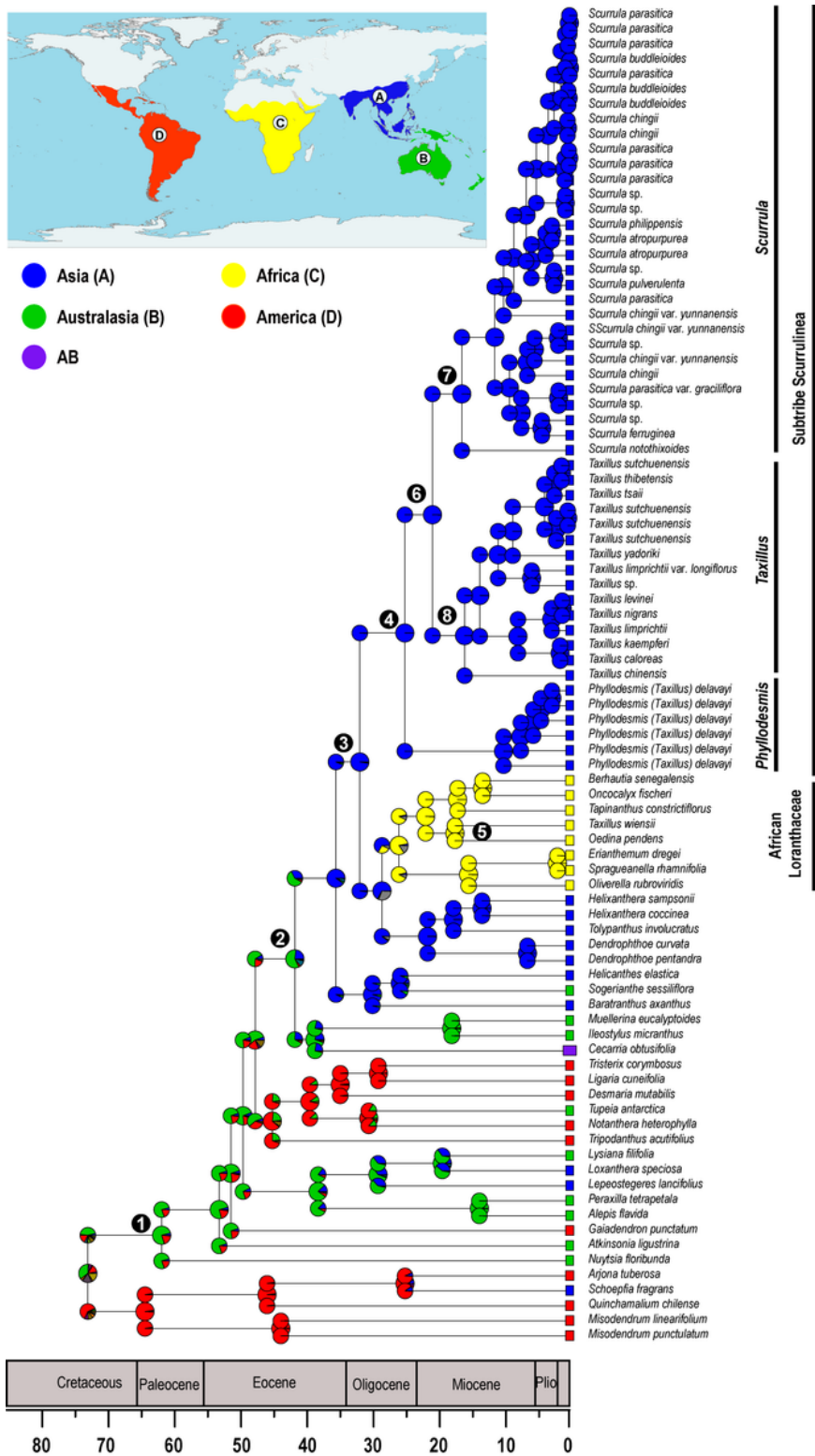


Figure 6

Ancestral area reconstruction of Scurrulinae by BioGeoBEARS ($j = 0.0169$, $\text{LnL} = -48.35$). Geologic time scale is shown at the bottom. Numbers outside nodes correspond to the node numbers in Fig. 5. Area abbreviations are as follows: A = Asia (including mainland of South Asia, Indochina and Malesia, but excluding New Guinea); B = Australasia (including Australia, New Zealand, New Guinea, and Pacific

Islands); C = Africa (including the coastal area of the Arabian Peninsula and Sub-Saharan Africa); D = Americas (including Mexico, Central and South America).

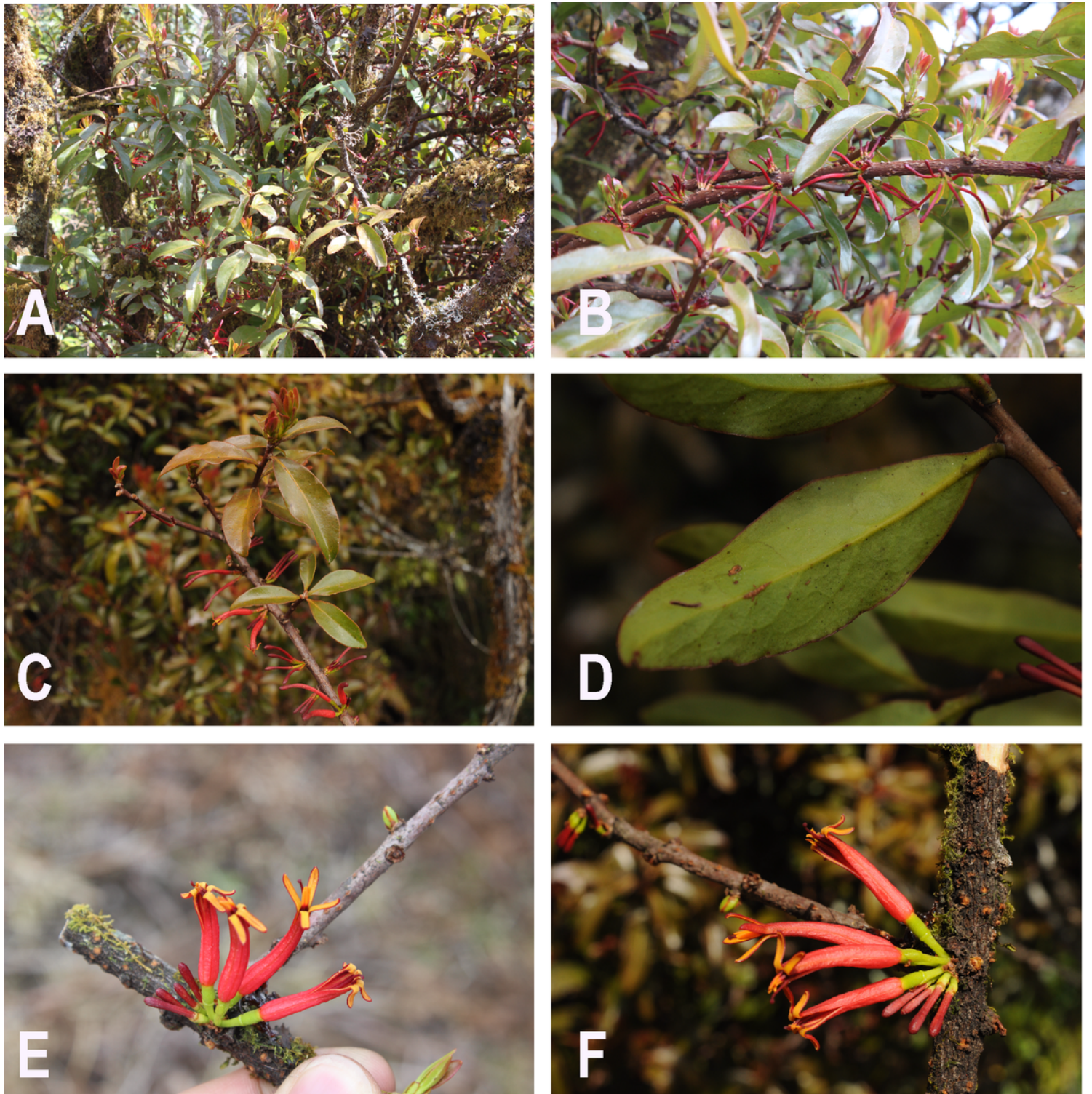


Figure 7

The morphological characters of *Phyllodesmis delavayi*. A – B: habits; C: adaxial leaf; D: abaxial leaf; E – F: inflorescence and flower. Photo credits: C. T. Le.

Supplementary Files

This is a list of supplementary files associated with this preprint. Click to download.

- [FigureS1.tif](#)
- [Supplementarymaterial.docx](#)